Synthesis of a novel HER2 targeted aza-BODIPY–antibody conjugate: Synthesis, photophysical characterisation and *in vitro* evaluation.

Miffy. H. Y. Cheng,[a] Antoine Maruani,[b] Huguette Savoie,[a] Vijay Chudasama[b*] and Ross. W. Boyle[a*]

[a.] *School of Mathematics and Physical Sciences, University of Hull, Cottingham road, Hull, UK, HU6 7RX*

[b.] *Department of Chemistry, University College London, London, UK.*

[*]*Joint corresponding authors.*

Contents

1. NMRs and MSs

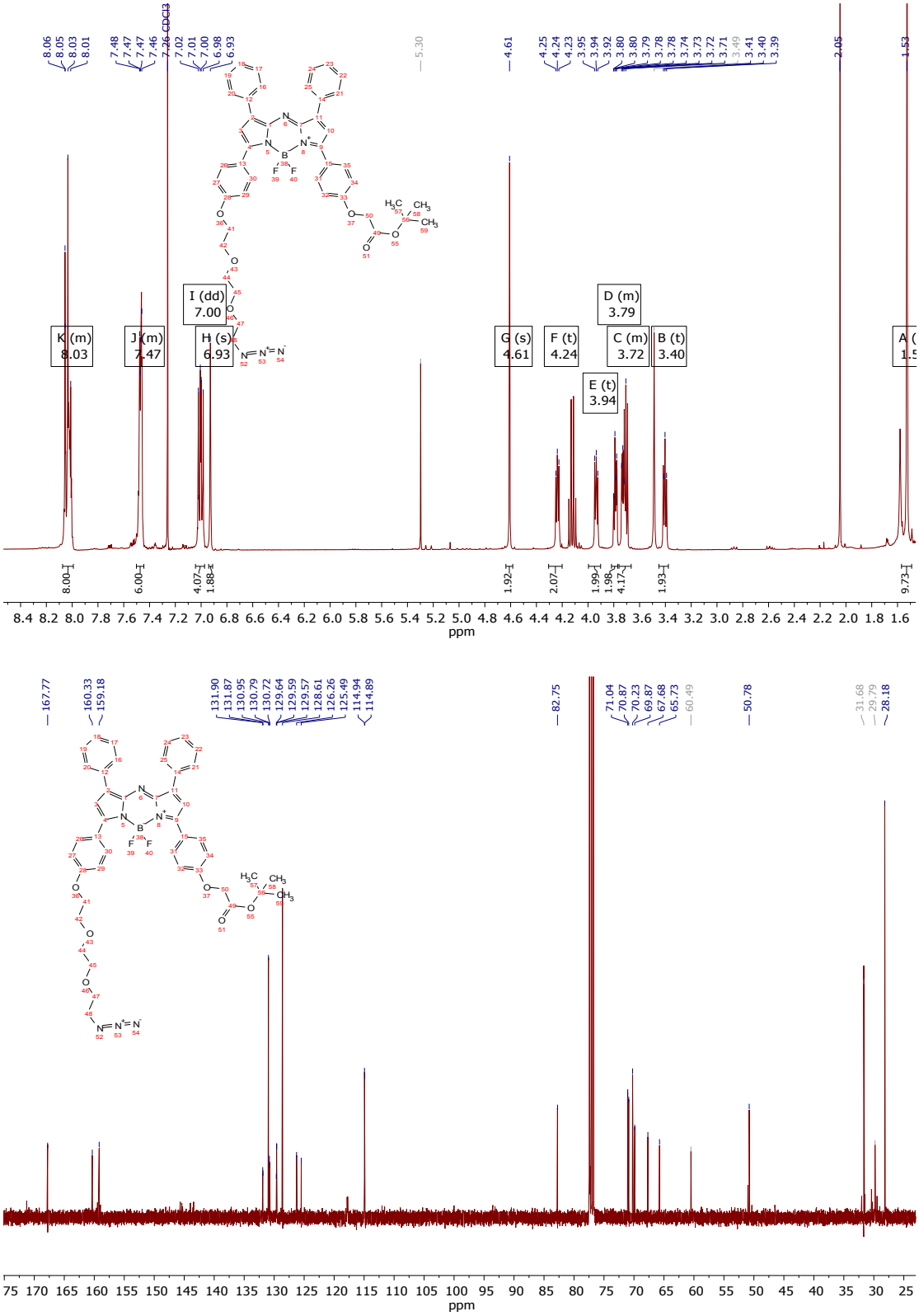

Figure S1. ^{1}H and ^{13}C NMR data for *tert*-butyl 2-(4-(7-(4-(2-(2-(2-azidoethoxy)ethoxy)ethoxy)phenyl)-5,5-difluoro-1,9-diphenyl-5*H*-4l4,5l4-dipyrrolo[1,2-c:2',1'-f][1,3,5,2]triazaborinin-3-yl)phenoxy)acetate (**2**)

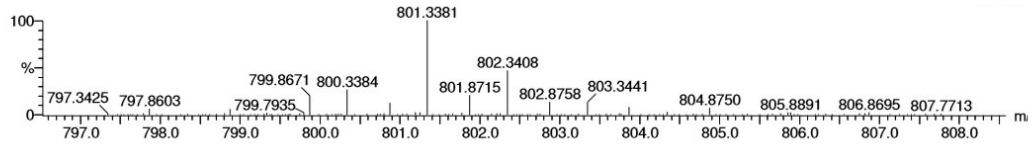

Minimum:				−150.0				
Maximum:		5.0	5.0	100.0				
Mass	Calc. Mass	mDa	PPM	DBE	i-FIT	Norm	Conf(%)	Formula
801.3381	801.3383	−0.2	−0.2	25.5	486.0	6.353	0.17	C44 H44 N6 O6 F2 11B
	801.3383	−0.2	−0.2	31.0	486.7	7.061	0.09	C43 H38 N13 O F2 11B
	801.3378	0.3	0.4	38.0	492.0	12.328	0.00	C58 H42 N F2 11B
	801.3375	0.6	0.7	13.5	491.5	11.861	0.00	C28 H44 N14 O11 F2 11B
	801.3389	−0.8	−1.0	13.0	490.4	10.721	0.00	C30 H46 N11 O12 F2 11B
	801.3370	1.1	1.4	20.5	483.7	4.064	1.72	C43 H48 N2 O10 F2 11B
	801.3370	1.1	1.4	26.0	484.7	5.115	0.60	C42 H42 N9 O5 F2 11B
	801.3397	−1.6	−2.0	25.0	488.2	8.576	0.02	C46 H46 N3 O7 F2 11B
	801.3397	−1.6	−2.0	30.5	488.3	8.649	0.02	C45 H40 N10 O2 F2 11B
	801.3362	1.9	2.4	8.5	492.9	13.247	0.00	C27 H48 N10 O15 F2 11B
	801.3402	−2.1	−2.6	12.5	490.5	10.849	0.00	C32 H48 N8 O13 F2 11B
	801.3402	−2.1	−2.6	18.0	490.5	10.825	0.00	C31 H42 N15 O8 F2 11B
	801.3357	2.4	3.0	26.5	484.8	5.205	0.55	C40 H40 N12 O4 F2 11B
	801.3357	2.4	3.0	21.0	479.7	0.047	95.38	C41 H46 N5 O9 F2 11B
	801.3410	−2.9	−3.6	30.0	490.6	10.979	0.00	C47 H42 N7 O3 F2 11B
	801.3352	2.9	3.6	33.5	492.7	13.099	0.00	C55 H44 O3 F2 11B
	801.3410	−2.9	−3.6	24.5	490.8	11.149	0.00	C48 H48 O8 F2 11B
	801.3348	3.3	4.1	9.0	494.9	15.241	0.00	C25 H46 N13 O14 F2 11B
	801.3415	−3.4	−4.2	12.0	491.1	11.467	0.00	C34 H50 N5 O14 F2 11B
	801.3415	−3.4	−4.2	17.5	490.7	11.117	0.00	C33 H44 N12 O9 F2 11B
	801.3343	3.8	4.7	21.5	484.3	4.648	0.96	C39 H44 N8 O8 F2 11B
	801.3343	3.8	4.7	16.0	485.1	5.421	0.44	C40 H50 N O13 F2 11B
	801.3343	3.8	4.7	27.0	487.3	7.671	0.05	C38 H38 N15 O3 F2 11B

Figure S2. MS data for *tert*-butyl 2-(4-(7-(4-(2-(2-(2-azidoethoxy)ethoxy)ethoxy)phenyl)-5,5-difluoro-1,9-diphenyl-5*H*-4l4,5l4-dipyrrolo[1,2-c:2',1'-f][1,3,5,2]triazaborinin-3-yl)phenoxy)acetate (**2**)

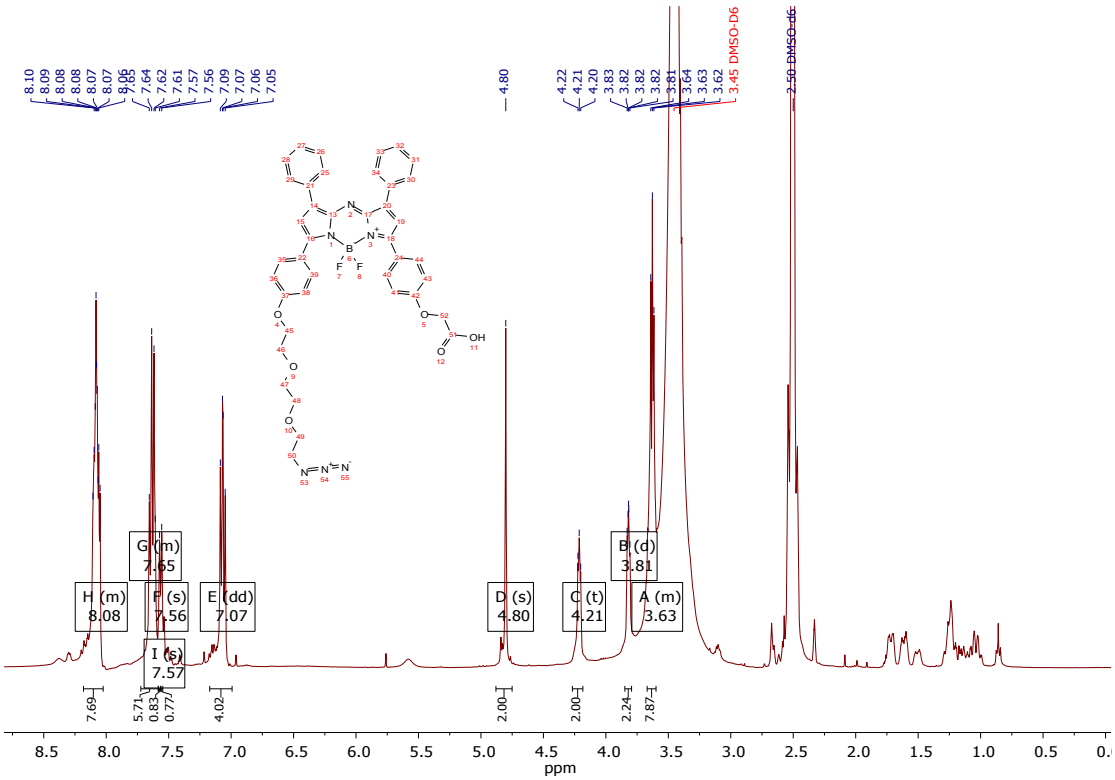
8.10
8.09
8.08
8.08
8.07
8.07
7.64
7.62
7.61
7.57
7.56
7.09
7.07
7.06
7.05
4.80
4.22
4.21
4.20
3.83
3.82
3.82
3.82
3.81
3.64
3.63
3.62
3.45 DMSO-D6
2.50 DMSO-d6
G (m) 7.65
H (m) 8.08
F (s) 7.56
E (dd) 7.07
I (s) 7.57
D (s) 4.80
C (t) 4.21
B (d) 3.81
A (m) 3.63
7.69
5.71
0.83
0.77
4.02
2.00
2.00
2.24
7.87
ppm

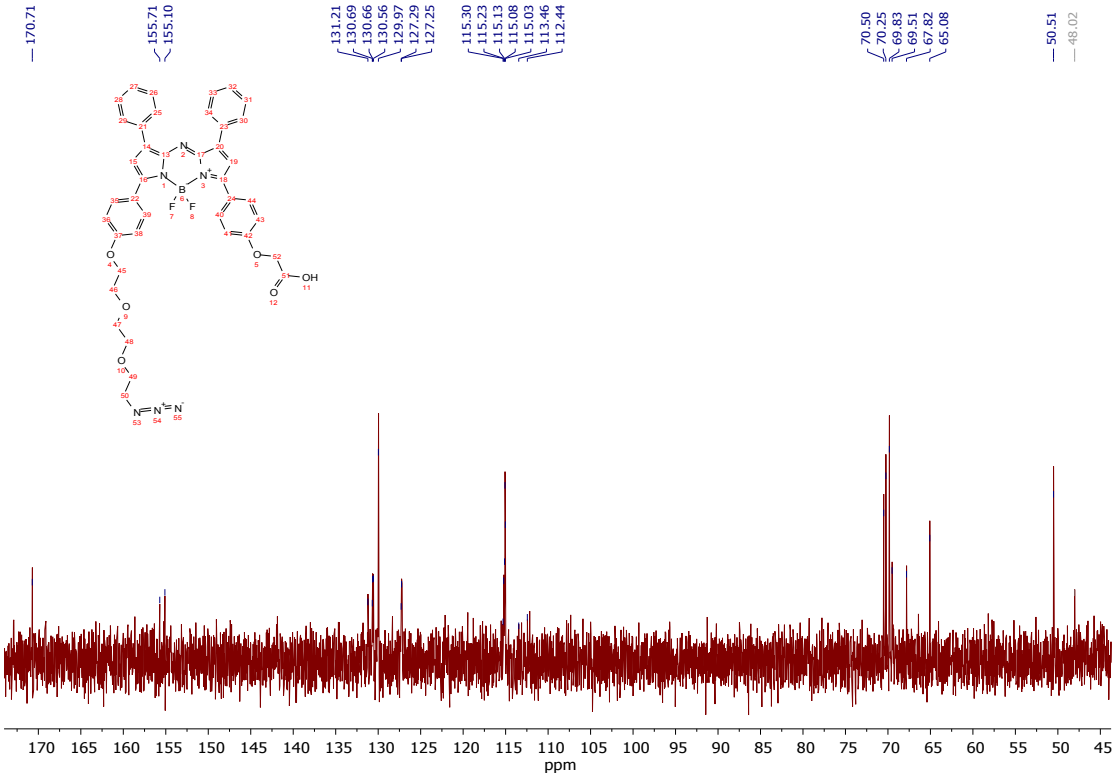
170.71
155.71
155.10
131.21
130.69
130.66
130.56
129.97
127.29
127.25
115.30
115.23
115.13
115.08
115.03
113.46
112.44
70.50
70.25
69.83
69.51
67.82
65.08
50.51
48.02
ppm

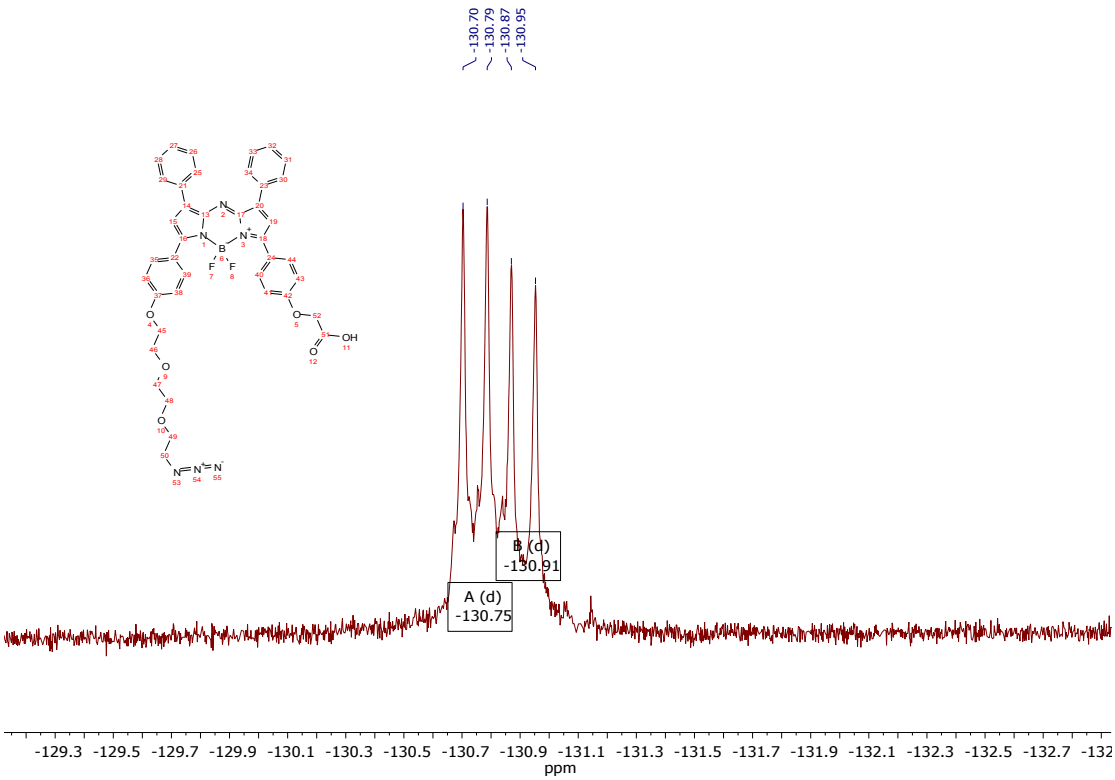

Figure S3. ^{1}H, ^{13}C and ^{19}F NMR data for 2-(4-(7-(4-(2-(2-(2-azidoethoxy)ethoxy)ethoxy)phenyl)-5,5-difluoro-1,9-diphenyl-5*H*-4l4,5l4-dipyrrolo[1,2-c:2',1'-f][1,3,5,2]triazaborinin-3-yl)phenoxy)acetic acid (**3**)

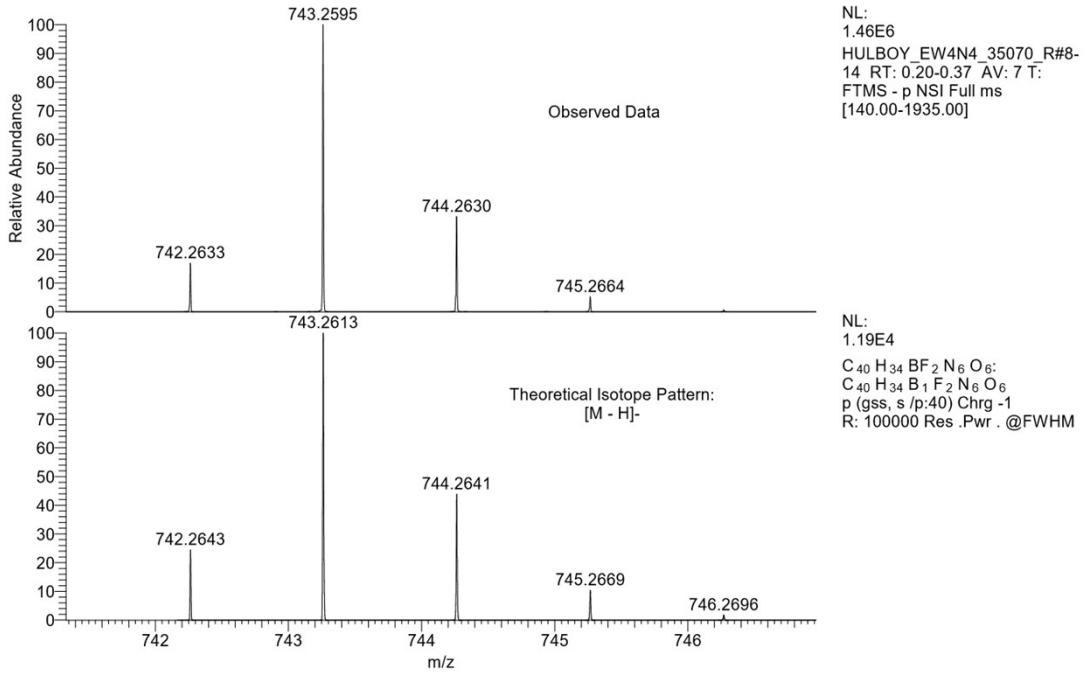

Figure S4. MS data for 2-(4-(7-(4-(2-(2-(2-azidoethoxy)ethoxy)ethoxy)phenyl)-5,5-difluoro-1,9-diphenyl-5*H*-4l4,5l4-dipyrrolo[1,2-c:2',1'-f][1,3,5,2]triazaborinin-3-yl)phenoxy)acetic acid (**3**)

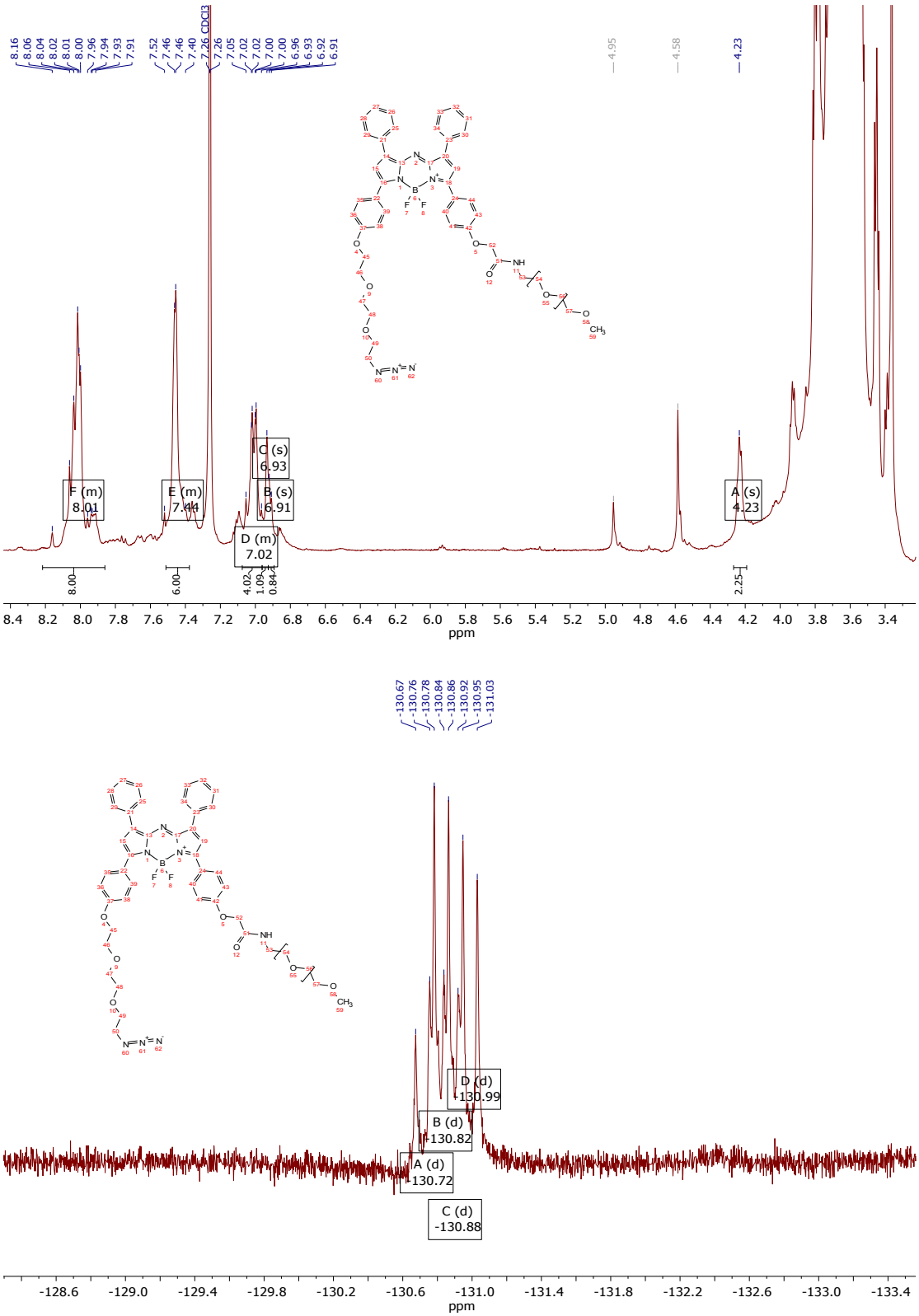

Figure S5. ^{1}H and ^{19}F NMR data for 2-(4-(7-(4-(2-(2-(2-azidoethoxy)ethoxy)ethoxy)phenyl)-5,5-difluoro-1,9-diphenyl-5*H*-4l4,5l4-dipyrrolo[1,2-c:2',1'-f][1,3,5,2]triazaborinin-3-yl)phenoxy)acetic acid (**3**)

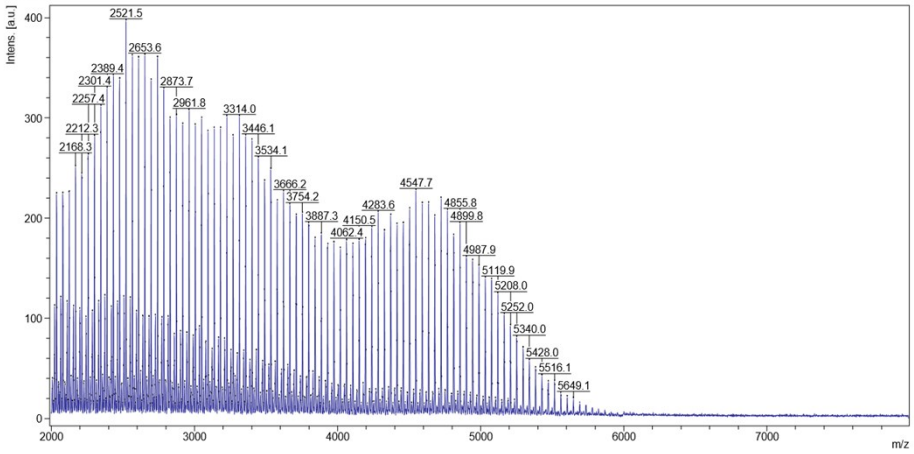

Figure S6. MALDI data in positive-linear mode for2-(4-(7-(4-(2-(2-(2-azidoethoxy)ethoxy)ethoxy)phenyl)-5,5-difluoro-1,9-diphenyl-5*H*-4l4,5l4-dipyrrolo[1,2-c:2',1'-f][1,3,5,2]triazaborinin-3-yl)phenoxy)acetic acid (**3**)

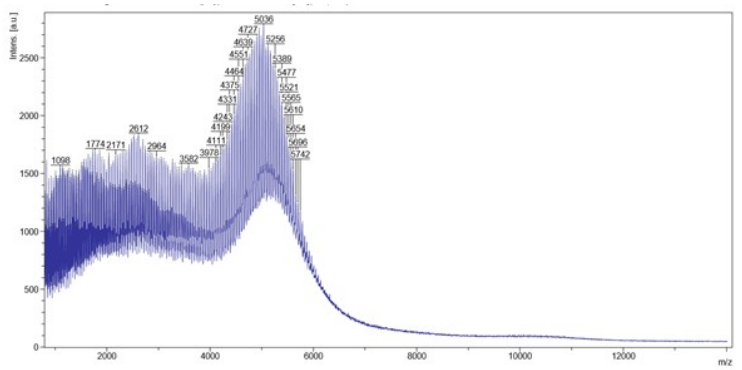

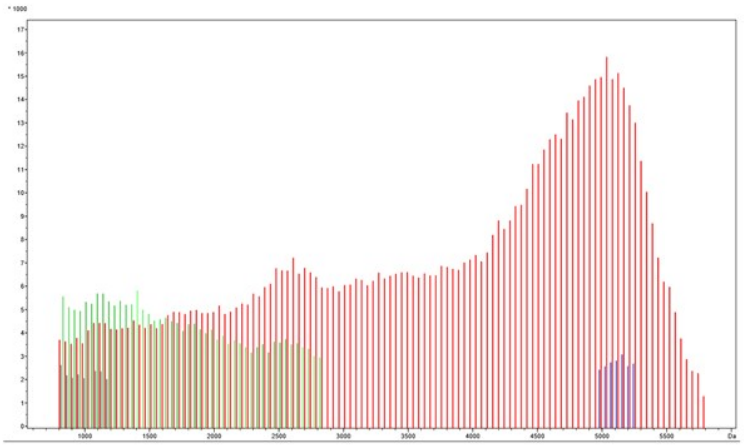

n	ser.	rep.unit	resid.	end1	end2	cation	Mn	Mw	pd	DP	% I.	cnt
1	1	PEG	33.9235			Na	3679.30	4169.26	1.13317	83.5206	77.3	114
2	2	PEG	20.0815			Na	5088.67	5090.10	1.00028	115.513	1.8	7
3	3	PEG	18.0989			Na	1698.43	1894.29	1.11532	38.5545	19	46

Figure S7. MALDI data in reflectron mode for2-(4-(7-(4-(2-(2-(2-azidoethoxy)ethoxy)ethoxy)phenyl)-5,5-difluoro-1,9-diphenyl-5*H*-4l4,5l4-dipyrrolo[1,2-c:2',1'-f][1,3,5,2]triazaborinin-3-yl)phenoxy)acetic acid (**3**)

2. Analysis of conjugate 8

UV-Vis spectra were recorded on a Varian Cary 100 Bio UV/Visible spectrophotometer, operating at room temperature. Sample buffer was used as blank for baseline correction. Calculation of molecule over antibody ratio, *r*, follows the formula below with ε_{280} = 215380 M^{-1} cm^{-1} for trastuzumab, ε_{345} = 9100 M^{-1} cm^{-1} for Mestra-PD, ε_{635} = 23442 M^{-1} cm^{-1} for the aza-BODIPY, 0.11 as a correction factor (CF) for Mestra-PD for the absorbance at 280 nm and 0.29 for aza-BODIPY at 635 nm.

$$r = \frac{A_\lambda/\varepsilon_\lambda}{\left(A_{280} - \sum CF_\lambda \times A_\lambda\right)/\varepsilon_{280}}$$

With A_λ the absorbance at the wavelength λ, and ε_λ extinction coefficient of the relevant molecule.

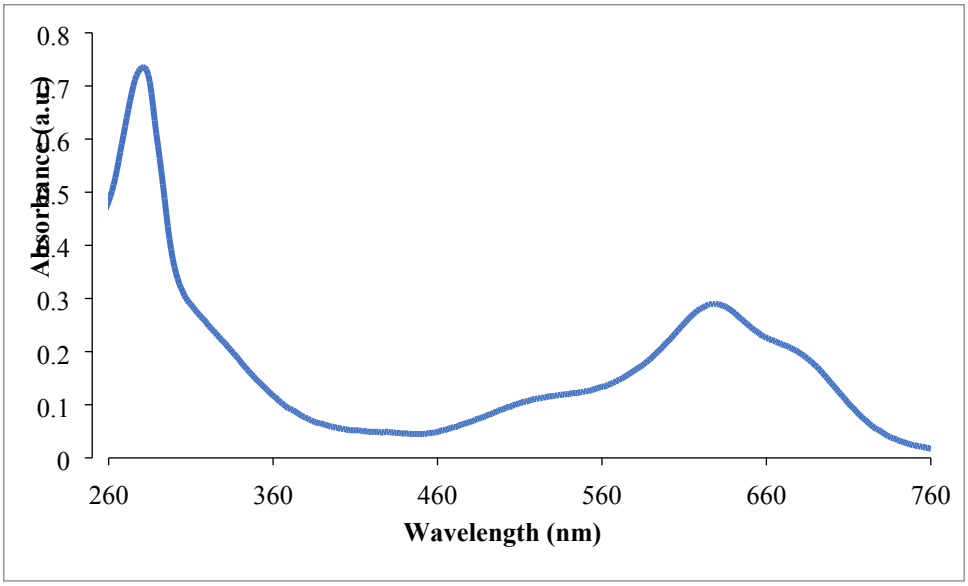

Figure S8. UV-Vis spectrum of conjugate **8**, showing absorption bands relating to aza-BODIPY, and trastuzumab rebridged with **5**.

Table 1. Photophysical properties of aza-BODIPY **4** at 298 K.

Compound	Solvent	λ_{abs}(nm)	λ_{em}(nm)	ε (L mol^{-1} cm^{-1})	Φ_f
4	Water	645	713	23442	0.19

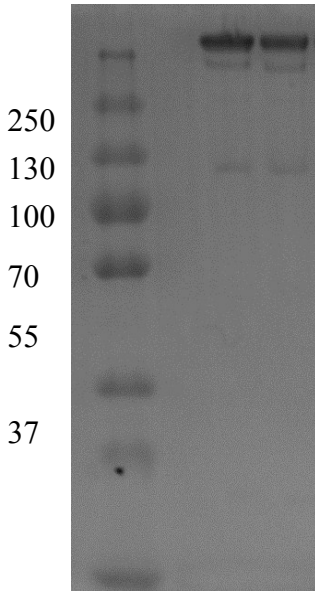

Figure S9. SDS-PAGE of (from left to right): ladder / trastuzumab rebridged with **5** / conjugate **8**.

3. Cell preparation and confocal Imaging

MDA-MB-468 (1×10^4 cells/mL) in DMEM-HG and BT-474 cells (2×10^4 cells/mL) in DMEM-F12 were seeded into 35 mm glass base dishes and left to attach overnight. The media was then removed and 5 μM of the conjugates **5** was added and incubated at 4 °C for 30 min. The diluted conjugate was removed, the cells were washed with PBS and fresh complete medium added before live cell imaging on the confocal microscope. The laser used was adapted to the absorption maximum of the conjugate (HeNe 633 nm laser). Cells were monitored for signs of necrosis or apoptosis, but none were detect under the conditions used for imaging.

3.1 Z-stacking CLSM images of both breast cancer cell lines

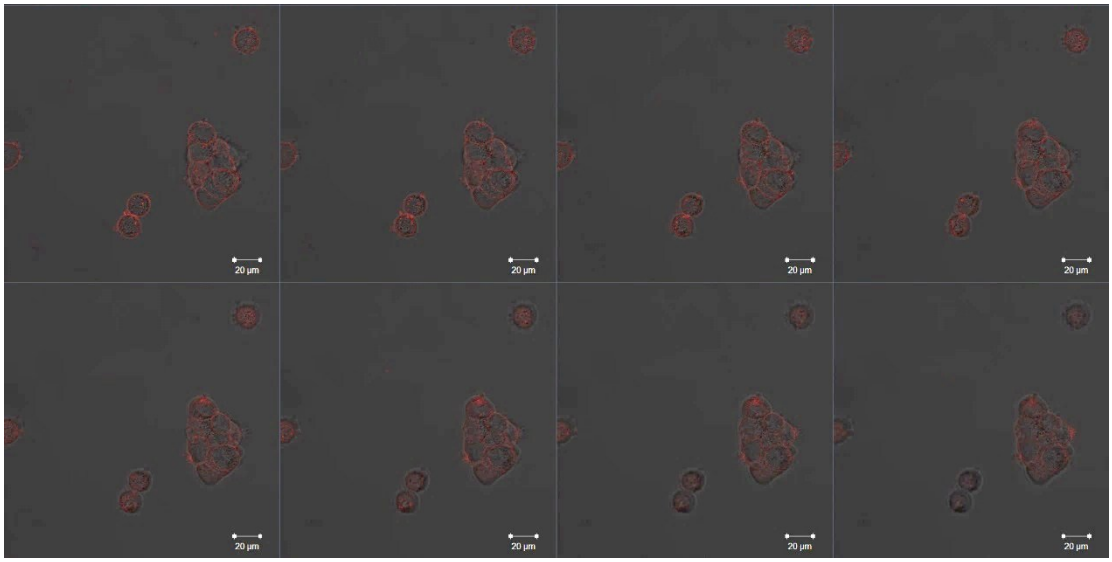

Figure S10. Z-stack images following 30 min incubation at 4 °C of **8** with BT-474 (HER2+) cells. Excitation at 633 nm with HeNe laser.

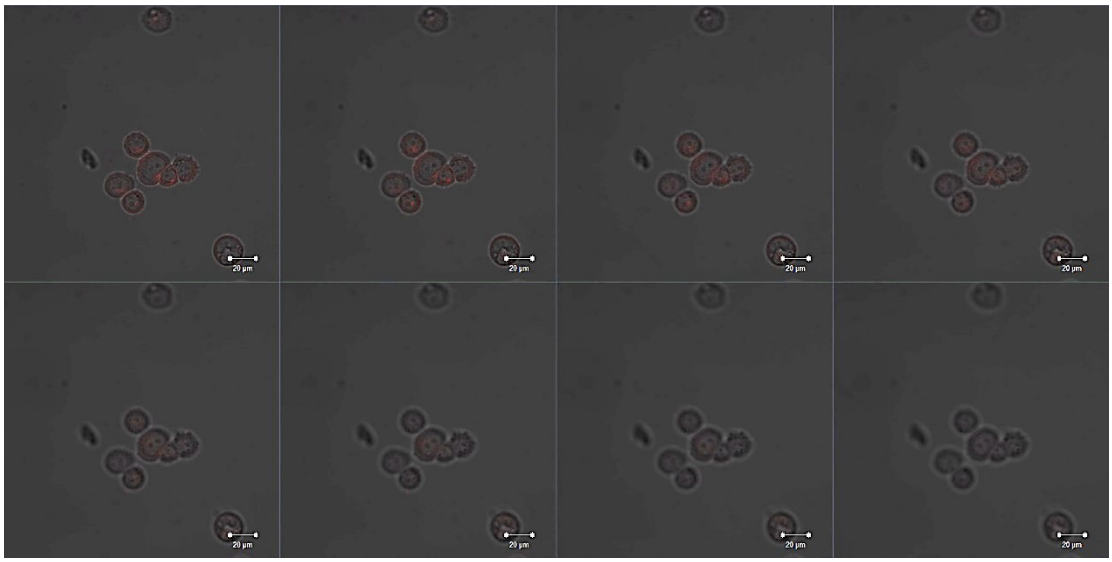

Figure S11. z-stack images following 30 min incubation at 4 °C of **8** with MDA-MB-

468 (HER2-) cells. Excitation at 633 nm with HeNe laser.

4. Total corrected cellular fluorescence

Using ImageJ, an outline was drawn around each cell and circularity, area, mean fluorescence measured, along with several adjacent background readings (n=3). The total corrected cellular fluorescence (TCCF) was calculated using following equation[6]:

$$TCCF = \bar{x}\, ID - (\bar{x}\, ASC \times \bar{x}\, MFBR)$$

ID is integrated density, *ASC* is area of selected cell and *MFBR* is mean fluorescence of background readings. This TCCF was then equalized against the mean TCCF of neighbouring interphase cells in the same field of view, with results presented as relative fluorescence over background and TCCF were compared between two breast cancer cell lines incubated with **8**.

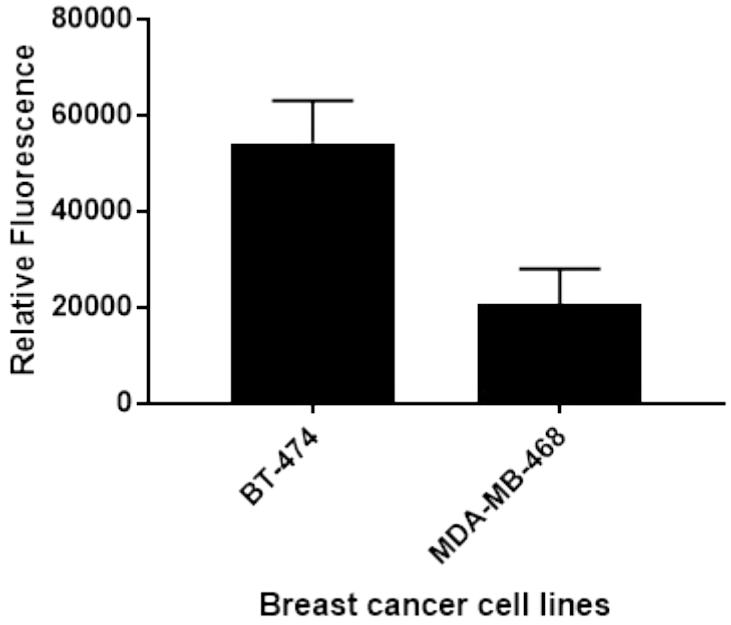

Figure S12. Calculated total corrected cellular fluorescence (TCCF) from confocal image of BT-474 (HER2+) and MDA-MB-468 (HER2-) cells incubated with **8**.

5. References

1 D. B. G. Williams and M. Lawton, *J. Org. Chem.*, 2010, **75**, 8351–8354.

2 A. Maruani, H. Savoie, F. Bryden, S. Caddick, R. Boyle and V. Chudasama, *Chem. Commun.*, 2015, **51**, 15304–15307.

3 A. M. Brouwer, *Pure Appl. Chem.*, 2011, **83**, 2213–2228.

4 J. R. Lakowicz, *Principles of Fluorescence Spectroscopy*, Kluwer Academic/Plenum Publishers, 2nd Ed., 1999.

5 D. Magde, G. E. Rojas and P. G. Seybold, *Photochem Photobiol*, 1999, **70**, 737–744.

6 R. A. Mccloy, S. Rogers, C. E. Caldon, T. Lorca, A. Burgess, R. A. Mccloy, S. Rogers, C. E. Caldon, T. Lorca, R. A. Mccloy, S. Rogers, C. E. Caldon, T. Lorca, A. Castro and A. Burgess, *Cell Cycle*, 2014, **13**, 1400–1412.